Low Temperature Physics/Fizika Nizkikh Temperatur, 2019, v. 45, No. 3, pp. 395–403

The low-temperature specific heat of MWCNTs

V.V. Sumarokov[1], A. Jeżowski[2], D. Szewczyk[2], M.I. Bagatski[1], M.S. Barabashko[1,3], A.N. Ponomarev[4], V.L. Kuznetsov[5,6], and S.I. Moseenkov[5]

[1]*B. Verkin Institute for Low Temperature Physics and Engineering of the National Academy of Sciences of Ukraine*
47 Nauky Ave., Kharkiv 61103, Ukraine
E-mail: sumarokov@ilt.kharkov.ua

[2]*W. Trzebiatowski Institute of Low Temperature and Structure Research, Polish Academy of Sciences*
P.O. Box 1410, Wroclaw 50–950, Poland

[3]*National Research Tomsk Polytechnic University, 30 Lenin Ave., Tomsk 634050, Russia*

[4]*Institute of Strength Physics and Materials Science of SB RAS, 2/4 Academicheskii Ave., Tomsk 634055, Russia*

[5]*Boreskov Institute of Catalysis, 5 Lavrentiev Ave., Novosibirsk 630090, Russia*

[6]*National Research Tomsk State University, 36 Lenin Ave., Tomsk 634050, Russia*

Received December 17, 2018

The specific heat of multi-walled carbon nanotubes (MWCNTs) with a low defectiveness and with a low content of inorganic impurities has been measured in the temperature range from 1.8 to 275 K by the thermal relaxation method. The elemental composition and morphology of the MWCNTs were determined using scanning electron microscopy analysis and energy dispersion x-ray spectroscopy. The MWCNTs were prepared by chemical catalytic vapor deposition and have mean diameters from 7 nm up to 18 nm and lengths in some tens of microns. MWCNTs purity is over 99.4 at.%. The mass of the samples ranged from 2–4 mg. It was found that the temperature dependence of the specific heat of the MWCNTs differs significantly from other carbon materials (graphene, bundles of SWCNTs, graphite, diamond) at low temperatures. The specific heat of MWCNTs systematically decreases with increasing diameter of the tubes at low temperatures. The character of the temperature dependence of the specific heat of the MWCNTs with different diameters demonstrates the manifestation of different dimensions from 1D to 3D, depending on the temperature regions. The crossover temperatures are about 6 and 40 K. In the vicinity of these temperatures, a hysteresis is observed.

Keywords: carbon nanotubes, MWCNTs, specific heat, low-dimensional systems.

Introduction

The discovery of carbon nanosystems (fullerenes, SWCNTs, MWCNTs, graphene) led to a great interest in both fundamental science and for applied purposes [1–9]. This is due to the peculiarities of their structures and unusual physico-chemical properties. In particular, MWCNTs are suitable objects for studying the physical properties of low-dimensional systems. Carbon nanotubes have also attracted great attention due to their potential technological applications (nanoelectronics, construction materials, pharmaceuticals, medicine, etc.) [10].

MWCNT is an isolated multi-layer roll of a graphene sheet or a set of coaxial SWCNTs in the form of a Russian nesting doll (Fig. 1). Between the layers, there is a weak van der Waals bond. The average diameter of MWCNTs is from a few to 100 nm. The distance between the atomic graphene layers is about 0.34 nm as in graphite [3]. The nanotube SWCNT is an elongated cylinder consisting of

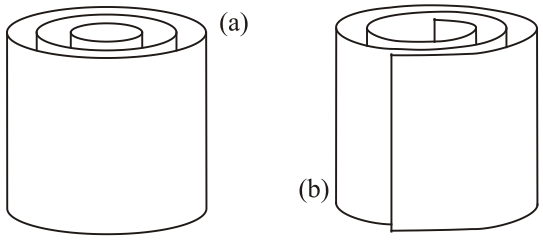

Fig. 1. Schematic sketch of the most common MWCNTs. Their multi-layered structure is a single-layer nanotube, “dressed” one by one according to the principle of Russian nesting dolls (a) or rolled up into a scroll of graphene sheet (b).

equilateral hexagons with carbon atoms at their vertices. This is a graphene plane rolled into a tube.

The physical properties of MWCNTs (in particular, thermal properties) depend on the methods and technology of tube preparation, their morphology, and the presence of impurities and defects. Usually, multi-walled carbon nanotubes are prepared by CVD (chemical vapor deposition) or AD (arc discharge) method with different catalysts, using different technological procedures: temperature regimes, purification methods, etc.

Studies of the specific heat of MWCNTs were carried out by both experimental and theoretical methods. Yi *et al.* [11] measured the specific heat and thermal conductivity of the small array like samples of highly aligned MWCNTs (1–2 mm long, with a cross-sectional diameter of 0.01–0.1 mm) by the self-heating 3ω method. The diameter of the MWCNTs was a few tens of nm, the walls of the nanotubes contained 10–30 layers. They found that the specific heat varies linearly in the temperature range of 10–300 K. The authors note that because of the uncertainty of the number of MWCNTs in array-like samples, the absolute values of the thermal conductivity coefficient (and, hence, the heat capacity determined with its help) suffer from uncertainty.

Mizel *et al.* [12] used to study the specific heat of pressed small cylindrical samples of MWCNTs (tubes were with outer diameters of order 10–20 nm and lengths exceeding 10 μm) weighing 10–20 mg with a diameter of 3.2 mm a thermal relaxation technique from 0.6 K up to 210 K. The analysis showed that the $C(T)/T^2$ curves for MWCNTs and graphite coincide above 50 K. The curve $C(T)/T^2$ for graphite has a maximum at 40 K. The $C(T)/T^2$ dependence for the MWCNTs exceeds it for graphite below 40 K. And the maximum of the MWCNTs curve shifts toward helium temperatures. The similarity between $C(T)/T^2$ for multi-walled tubes and for graphite indicates that the two materials are similar.

Masarapu *et al.* [13] measured the specific heat of aligned multi-walled carbon nanotubes (obtained by CVD method with diameters in the range of 20–30 nm and consisting of 15–25 layers) in the temperature range from 1.8 to 250 K. They found that in the range of 40–250 K there is a linear dependence of the specific heat. Below 40 K, the specific heat gradually decreases, demonstrating a change in dimension from 1D to 3D behavior, indicated by different temperature dependences at low temperature. This behavior of the heat capacity was attributed to a dimensional change in the density of states from 3D at low temperatures to a reduced dimension at higher temperatures. Below 5 K, the T^{-2} feature due to magnetic impurities was observed.

In the works of Jorge *et al.* [14,15], the specific heat of MWCNTs was measured in the range of 10–120 K. Samples with diameters of 90, 48 and 30 nm were obtained by the CVD method. They have an aligned nanotube structure and an internal bamboo-like structure within each MWCNT. The authors found an anomalous peak at 60 K in these samples. The parameters of the peak (height and temperature of the maximum) do not depend on the magnetic field and do not exhibit thermal hysteresis [15].

Authors [16] showed that taking into account the electron contribution to the heat capacity depending on the diameter of the nanotubes, the concentration of impurities, and short-range order parameters (structural inhomogeneities) allowed them to describe the peculiarities of low-temperature behavior of the experimental specific heat of MWCNTs [15] with large diameters and an internal bamboo-like structure. However, according to Benedict *et al.* [17], the electron contribution to the heat capacity of pure carbon tubes is more than 100 times weaker than the phonon one.

Muratov *et al.* [18] using the adiabatic calorimetry method carried out measurements of the heat capacity of MWCNTs with an average diameter of less than 30 nm in the temperature range from 60 to 300 K. They observed the anomaly in heat capacity at temperatures of 80–90 K. The authors believe that it is similar to that observed at about 60 K in [14]. The samples with a diameter of 25 nm [14] and 17 nm [15], which were synthesized by the catalytic decomposition of acetylene over iron nanoparticles, had a forest distribution. The internal bamboo-like structure was absent in these samples. The dimensional behavior crossover (change from quasi-linear behavior to a higher dimension) was observed at 33 K for samples with a larger diameter of tubes and a bamboo-like internal structure and at 55 K for samples with diameters of 17 and 25 nm without a bamboo-like internal structure.

Popov [19] calculated the low-temperature specific heat of MWCNTs with different number n of layers within force-constant dynamical models. The specific heat curves of MWCNTs with n = 1–5 above 50–60 K coincide. At lower temperatures, the curves diverge. This discrepancy increases with decreasing temperature. At the same time, the degree of temperature dependence increases from 0.5 for n = 1 to 1 for n = 5.

Brief information about the samples (morphology and methods of preparation), methods and temperature ranges of measurement of heat capacity in the reviewed papers are presented in the Table 1.

The discrepancies between the experimental values of the specific heats of different works may be due to differences in purity, in structure, in structural defects and heterogeneities, in the diameters and quantities of the layers in the MWCNTs samples and systematic errors. Systematic errors are mainly caused by the presence of carbonic and other impurities in the samples: gaseous helium (sometimes used to cool the calorimetric cell), catalyst residues, atmospheric gases and other impurities. The authors [16,20–24] showed that electron scattering by impurities and structural inhomogeneities, such as non-uniformity of the short-range order, can lead to anomalous behavior of both the thermal, transport and electron properties of carbon nanomaterials.

Table 1. Brief information about the samples

Ref.	Synthesis technique	Average diameter, nm (length)	Temperature interval, K	Measuring technique	Sample mass
[12]	AD[1]	10–20 (10 μm)	1–200	Thermal relaxation technique	10–20 mg
[11]	CVD[2]	20–40	10–300	Self-heating 3ω method	
[15]	CVD[2]	Sample A1 ∅90[3]/∅58[4]	6–120	Relaxation method	200 μg
	CVD[2]	Sample B ∅48[3]/∅21[4]			
		Sample C ∅17[3]/∅5[4]			
[18]	CVD[2]	below 30	56–300	Adiabatic technique	
[13]	CVD[2]	20–30 (1–3 mm)	1.8–250	Relaxation technique	2.2 mg

Notes: [1] arc discharge technique, [2] chemical vapor deposition, [3] outer diameter of MWCNTs, [4] inside diameter of MWCNTs.

In Hone's study [25], it was found that the presence of helium in bundles of SWCNTs leads to an anomalous behavior of the specific heat below 20 K (see Fig. 2 in Ref. 25). Adsorbed Xe, N_2, and CH_4 impurities lead to a significant increase in the specific heat of bundles of closed single-wall carbon nanotubes at low temperatures [26–30]. For example, the concentration of several admixture nitrogen molecules per 1000 carbon atoms in bundles of single-walled carbon nanotubes leads to an increase in the specific heat by a factor of 1.5 at ~ 2 K. Thus, thorough cleaning of samples from gas impurities is an integral part of obtaining precision data on the heat capacity of carbon nanomaterials.

In the reviewed papers, MWCNTs were obtained using different methods and technologies. The analysis of the discussed results is difficult due to the lack of complete information in a number of papers on the purity of MWCNTs, measurement errors, etc. The results of measurements of the specific heat vary greatly; especially in the low-temperature region (see below Fig. 6). Despite intensive experimental studies, the specific heat at constant pressure of multilayer carbon nanotubes has not been comprehensively studied at low temperatures. Also, interest in carbon nanotubes from the side of new applied problems requires more extensive studies of their properties depending on their size, production technology, and so on.

The present paper is devoted to studies of the low-temperature specific heat of multi-walled carbon nanotubes with a controlled level of defectiveness and with a low content of inorganic impurities in order to obtain information about the effects of dimensionality in the thermodynamics of MWCNTs with different diameters. We used the system set of MWCNTs, obtained using the same type of catalysts and defectiveness, which was characterized using TEM (transmission electron microscopy), Raman spectroscopy, XRF (x-ray fluorescence method), EDS (the energy dispersive x-ray spectroscopy), and temperature dependence of conductivity [31–37].

Experiment

The calorimetric studies of MWCNTs have been made in the temperature range from 1.8 to 275 K. The specific heat was measured using the thermal relaxation method. The measurements were carried out on the physical property measurement system (PPMS) from Quantum Design Inc. operating in the heat capacity mode. A simplified draft of the set-up is shown in Fig. 2 [38].

Measuring system (the so-called puck) consist of a measuring platform on which a sample is anchored with an Apiezon grease. After mounting the sample on the puck, the chamber was sealed and cooled down to temperature 150 K. The measurements were carried out in high-vacuum conditions. Each time, two series of run were performed. During the first run measurements were performed from 150 K down to 2 K and from 2 K up to 275 K during the second one. The temperature of the sample was measured with the resistive thermometer Cernox (Lake Shore). The under consideration samples of MWCNTs were cut out from plates with thickness about 2–3 mm. The plates were obtained by compacting the MWCNTs powder under the pressure of 1.1 GPa as in Ref. 28.

MWCNTs were prepared using the CVD method by decomposition of ethylene over the bimetallic Fe-Co/Al_2O_3 catalyst at 670°C Fe_2Co as an active component [39,40]. This catalyst composition has been shown to provide MWCNTs of low defectiveness [31] and with low content

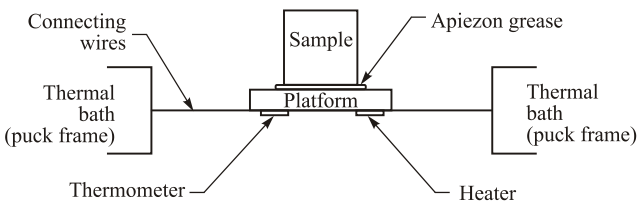

Fig. 2. Thermal connection scheme between a sample and the measuring platform in PPMS heat capacity puck.

Table 2. Chemical atomic composition of the MWCNTs samples

Sample	C at.%	O at.%	Si at.%	Cl at.%	Fe at.%	Cr at.%	Co at.%
s1	99.49	0.24	0.07	0.01	0.17	0.02	0
s2	99.45	0.31	0	0.04	0.04	0	0.03
s3	99.72	0	0	0.01	0.17	0.01	0.09

of inorganic impurities. Further refluxing of nanotubes with 15% HCl (followed by washing with distilled water until neutral pH and subsequent drying in air) allows decreasing the content of catalyst traces to 0.3–0.5 wt%. Purity of prepared MWCNTs powder is over 99.4 at.%. Information about the chemical composition of the samples is given in Table 2. In the experiment, 3 batches of MWCNTs powders differing in mean tube diameters were used: 7.2 nm (s1), 9.4 nm (s2) and 18 nm (s3). Information on the samples of the MWCNTs is given in Table 3. The morphology of MWCNTs with different diameters is visible in TEM images (Fig. 3). MWCNTs are not combined in bundles, unlike SWCNTs.

Table 3. Information about the MWCNTs samples

Sample	Mean diameter, nm	Length, nm	Mass, mg
s1	7.2	Up to 50000	2.35
s2	9.4	Up to 50000	2.37
s3	18	Up to 30000	4.3

Scanning electron microscopy (SEM) analysis was carried out on JEOL JSM-7500FA at 20 kV to evaluate surface morphology of the samples. Element composition and concentration were measured by the energy dispersive x-ray spectroscopy (EDS) [41].

The sample mass was specified with Sartorius CPA225D semi-microbalance. The mass of the samples was 2.35 mg (sample s1); 2.37 mg (sample s2) and 4.3 mg (sample s3) (see Table 3). During the experiment, the heat exchanging helium gas was not used for cooling of the calorimeter to the low temperatures.

Measurement error did not exceed 2%. Other details of the experiment were described elsewhere in Refs. 42, 43.

Results and discussion

The specific heat of MWCNTs with mean diameter of 7.2 nm (sample s1), 9.4 nm (s2) and 18 nm (s3) was measured in the temperature range from 2 to 275 K. The graphs of the temperature dependence of the specific heat of the studied samples are shown in Fig. 4. Figure 4 also displays the curves of the temperature dependence of the specific heat of graphene (theory) [25], bundles of SWCNTs (experiment) [26], graphite (experiment) [44–46] and diamond (experiment) [47,48].

It is noteworthy that the temperature dependences of the specific heat for all carbon materials discussed, with

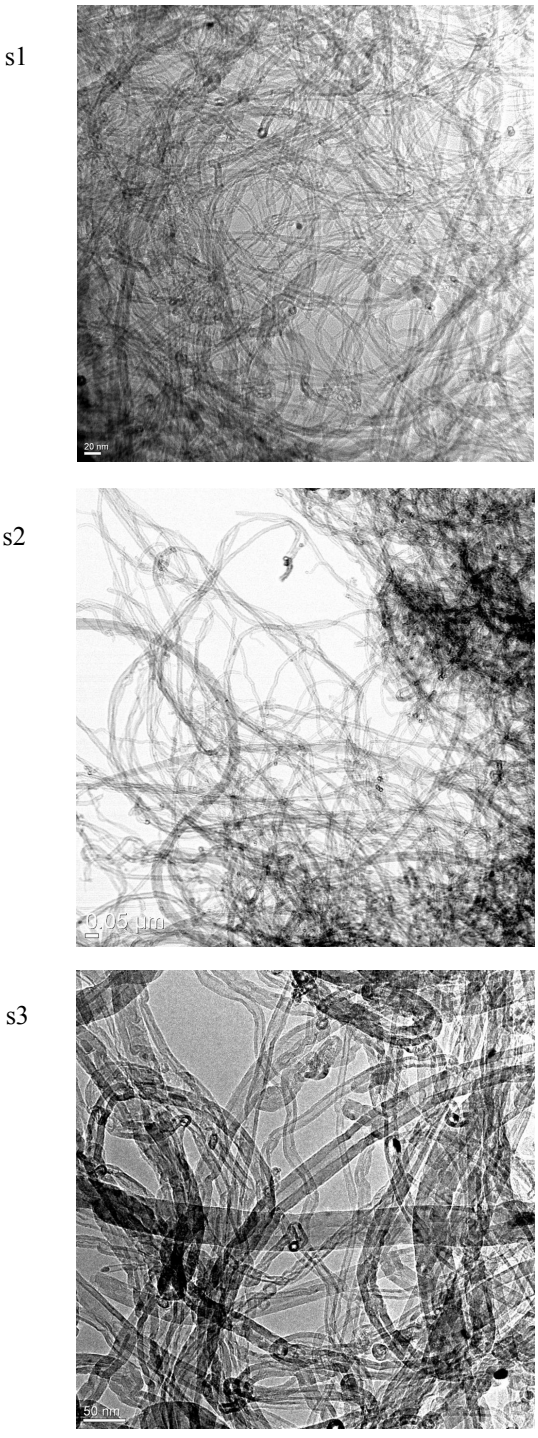

Fig. 3. The TEM images of MWCNTs with mean diameter 7.2 nm (s1), 9.4 nm (s2) and 18 nm (s3).

the exception of diamond, above 100 K are close: the difference in the results of studies does not exceed 15–30%. The curves begin to diverge below 60–100 K.

The behavior of the temperature dependence for diamond differs sharply from other carbon materials, which is apparently due to the fact that diamond has a sp^3 bond, in contrast to the different forms of the sp^2 bond for the remaining carbon materials. In diamond, carbon atoms are strongly bonded with the nearest neighbors (sp^3 hybridiza-

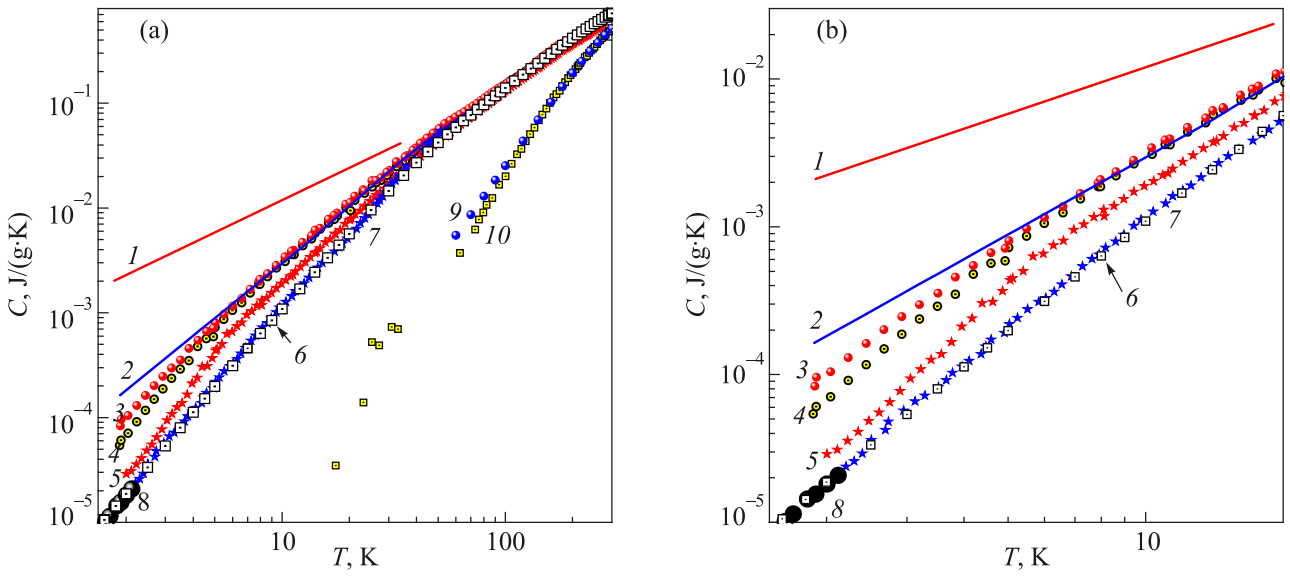

Fig. 4. (Color online) The temperature dependences of the specific heat of carbon materials. Theory: graphene [25] (*1*); Experiment: SWCNT bundles [26] (*2*); MWCNTs: the samples s1 (*3*); s2 (*4*); s3 (*5*) (present work); graphite: [44] (*6*), [45] (*7*); [46] (*8*); diamond [47] (*9*), [48] (10). (a) Entire temperature range; (b) Temperature range below 20 K.

tion); there are very high frequencies of vibrational modes and a high Debye temperature of about 2000 K [48].

In the allotropic forms of carbon: graphite, MWCNTs, and bundles of SWCNTs, there are both strong (sp^2 hybridization in the plane or on the nanotube surface) and weak (van der Waals) interactions between the layers and the walls of the tubes in bundles. The contribution of low-frequency modes to the heat capacity of these allotropic forms of carbon increases with decreasing temperature below 300 K. As a result, below 300 K, the difference between the temperature dependence curve of the heat capacity $C_P(T)$ of diamond and the curves of heat capacities $C_P(T)$ of graphite, graphene, MWCNTs, and SWCNT bundles increases with decreasing temperature.

The character of the low-temperature dependences of graphite, MWCNTs, and SWCNTs bundles is qualitatively similar, and the dimensionality effect in the heat capacity of these materials is determined by the relative contribution of low-frequency vibrations. In anisotropic layered graphite, carbon atoms form a hexagonal network and are connected by strong covalent "flat" bonds (sp^2 hybridization) [49,50]. The Debye temperature due to vibrations of carbon atoms in the plane is about ≈ 2500 K (higher than in diamond [51]). Between the layers, the carbon atoms are bound by weak van der Waals forces. At low temperatures, the contribution to the heat capacity of graphite from low-frequency vibrational modes dominates. From the analysis of low-temperature data on the heat capacity of graphite, Ramos *et al.* [45] found, that the Debye temperature is $\Theta_D \approx 420$ K, which is 5 times less than Θ_D diamond. In graphene, there are both high-frequency (vibrations of carbon atoms in the plane) and low-frequency (transverse vibrations) vibrational modes.

In the SWCNTs bundles, there are high-frequency vibrations of carbon atoms on the nanotube surface due to the strong interaction between carbon atoms (deformed sp^2 hybridization) and low-frequency vibrational modes (transverse vibrations of atoms, elastic longitudinal and torsional vibrations of the tube as a whole).

When the wavelength of the transverse oscillations is equal to or greater than the tube radius, the transverse radial modes are quantized [25]. Both in the SWCNTs and in multi-walled tubes, there is a weak interaction between the walls of the tubes due to the van der Waals forces.

The low-energy part of the spectrum will change with an increase in the number of tubes in bundles of SWCNTs and the number of walls in MWCNTs. According to the theory [19], an increase in the number of as single-walled tubes in the SWCNT bundles as and layers in multi-walled tubes leads to an increase in the frequency and a decrease in the density of states in the low-energy part of the spectrum. This reflects the trend observed in the experiments (present work and Refs. 12, 13).

The theoretical heat capacity curve for graphene [25] (Fig. 4) demonstrates a linear dependence on temperature and lies above the other curves below 60 K.

Above 6 K, the specific heat curves of MWCNTs (samples s1 and s2, diameters of tubes: 7.2 and 9.4 nm, respectively) and SWCNT bundles practically coincide. Below 6 K, the curves for MWCNTs (s1 and s2) diverge from the SWCNTs curve down towards graphite. Curves for MWCNTs sample s3 and for graphite noticeably diverge from curves of our samples s1 and s2 and graphene below 100 K. The curve for sample s3 with a tube diameter of 18 nm diverges from a graphite curve of about 30 K, below 30 K it lies higher than graphite curve, but below the curves s1 and s2.

Comparison of the obtained results with the literature data showed that at temperatures below 6 K the specific heat of MWCNTs decreases monotonically with an increase in the average diameter of the tubes (see below Fig. 6). The heat capacity curve MWCNTs (diameter 15 nm) from Ref. 12 is located between our curves for samples s2 (∅9.4 nm) and s3 (∅18 nm), and the curve (∅25 nm) from Ref. 13 lies below ours curve s3 (∅18 nm).

The results of Yi *et al.* [11], Jorge *et al.* [14,15] and Muratov *et al.* [18] are qualitatively close to each other. Below 60 K data of Yi *et al.* [11] and Jorge *et al.* [14,15] lie above both present results and the data from Refs. 12, 13. At 15 K, the data [11,14,15] exceed our results, the data from Ref. 12 (∅15 nm) and Ref. 13 (∅25 nm) more than 2 times. Note that the nature of such difference, apparently, is associated with a significant difference in the morphology of the tubes. The authors of [16] believe that this may be due to the manifestation of the electronic subsystem in the defective — "dirty" samples.

For convenience of analysis, let us present the temperature dependence of the MWCNTs specific heat of measured samples s1 (∅7.2 nm), s2 (∅9.4 nm) and s3 (∅18 nm) in coordinates C/T^2 vs T as are shown in Fig. 5. The nature of the temperature dependences of the heat capacity indicates the behavior with different dimensions in different temperature ranges. The curve s3 clearly shows how the behavior of $C(T)$ changes with temperature, corresponding to a change in dimensionality from linear at high temperatures to cubic at low temperatures through the quadratic at intermediate temperatures.

The nature of the temperature dependence of the specific heat of MWCNTs suggests that the manifestation of 1D–3D dimensionality is due to the competition between the contributions of low-frequency oscillations as in the tubes and between the walls of the tubes and high-frequency oscillations on the surface of the tubes in the density of phonon states. The dominant contribution is made by low-frequency oscillations between the walls of the tubes, as can be seen in the example of sample s3, in which the number of layers is noticeably larger than in the tubes of samples s1 and s2. The change in the behavior of the temperature dependence of the specific heat with a quasi-1D dimension to a quasi-2D is observed in the temperature range from about 40 to 200 K. The areas of crossovers are most brightly shown on sample s3 with a diameter of 18 nm: about 6 and about 40 K. Note that temperature hysteresis is observed in these areas. The quadratic temperature dependence of the specific heat is from 6 to 40 K. With the decrease of the diameter of the MWCNTs, the T^2-temperature dependence is blurred and the absolute values of the heat capacity increase.

At the same time, an analysis of the temperature dependences of the specific heats of literature data on graphite, SWCNT bundles, MWCNTs [12,13,26,44–46] shows that at the temperature close to 40 K a feature is observed — a crossover from quasi-1D to quasi-two-dimensional behavior (see Fig. 6). Neutron studies [52–54] show that the curves of the density of states for SWCNTs and graphite exhibit anomalies at energies of 2.5–3.5 meV and 16 meV (see Figs. 17–19 in Ref. 54 and Fig. 5 in Ref. 52), which correspond to the temperatures of the anomalies in heat capacity. Note that, as in the studies of heat capacity and thermal expansion [26], the temperature dependence of electrical conductivity [55] also exhibits a feature near 30 K. According to the authors of [55], this feature is due to

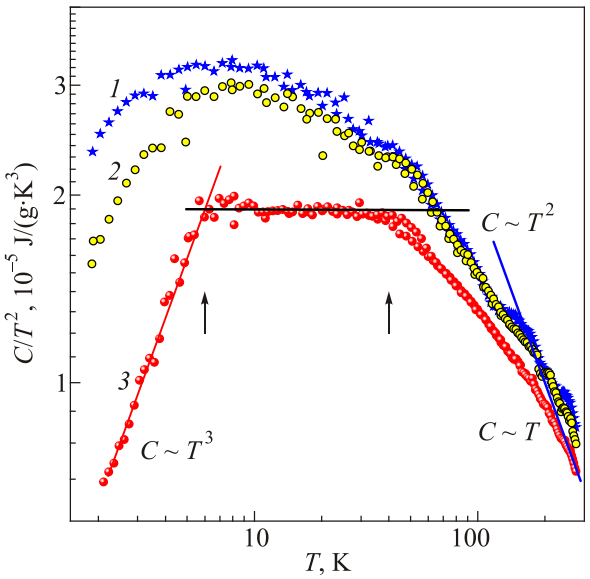

Fig. 5. (Color online) The specific heat of the studied samples s1 (*1*), s2 (*2*) and s3 (*3*) in coordinates C/T^2 vs T. Crossover temperatures are indicated by arrows.

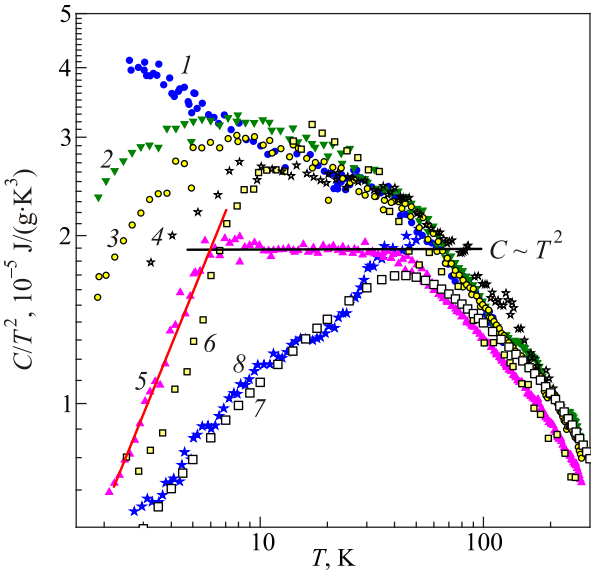

Fig. 6. (Color online) The specific heat in coordinates C/T^2 vs T: bundles of SWCNTs [26] (*1*); the MWSNT sample s1 (∅7.2 nm) (*2*); the MWSNT sample s2 (∅9.4 nm) (3); MWSNTs (∅ ~ 15 nm) [12] (*4*); the MWSNT sample s3 (∅18 nm) (*5*); MWSNTs (∅ ~ 25 nm) [13] (*6*); graphite: [44] (*7*), [45] (*8*).

the change in the mechanism of conductivity in a system oriented of SWCNTs from the state of the Luttinger liquid to the Mott dielectric phase in the temperature range 25–36 K. Also features in temperature dependences of conductivity (with diameters from 5.8 to 25 nm) and magnetoresistance (with diameters from 8.7 to 25 nm) MWCNTs (tubes similar to ours) were observed at temperatures below 50 K (see Fig. 2 in Ref. 32).

Conclusion

The specific heats of systematic set of MWCNTs with variable external diameters and number of graphene walls have been measured from 2 to 275 K by the thermal relaxation method. The elemental composition and morphology of the MWCNTs were determined using scanning electron microscopy analysis and energy dispersion x-ray spectroscopy. The MWCNTs prepared by chemical catalytic vapor deposition contained over 99.4 at.%, which have mean diameters from 7 nm up to 18 nm and lengths in some tens of microns. It was found that the low-temperature dependence of the specific heat of the MWCNTs of the studied samples differs significantly from other carbon materials (graphene, graphite, diamond) at low temperatures. It was also found that the specific heat of MWCNTs systematically decreases with increasing diameter of the tubes at low temperatures. The character of the temperature dependence of the specific heat of the MWCNTs samples with different diameters demonstrates the manifestation of different dimensionality from 1D to 3D, depending on the temperature regions. The crossover temperatures are about 6 and 40 K. In the vicinity of these temperatures, a temperature hysteresis is observed.

Acknowledgments

The authors thank Scientific and educational innovation center “Nanomaterials and nanotechnologies”, National Research Tomsk Polytechnic University for help in x-ray diffraction measurements and SEM-EDS analysis of the samples MWNCTs that were carried out within the framework of Tomsk Polytechnic University Competitiveness Enhancement Program.

1. A.V. Eletskii, *Usp. Phys. Nauk* **167**, 945 (1997) [*Phys. Usp.* **40**, 899 (1997)].
2. A.V. Eletskii, *Usp. Phys. Nauk* **179**, 225 (1997) [*Phys. Usp.* **52**, 209 (2009)].
3. M.S. Dresselhaus, *Carbon Nanotubes: Synthesis*, *Structure*, *Properties*, *and Applications*, Springer-Verlag (2000).
4. *Carbon Nanotubes: Science and Application*, M. Meyyappan (ed.), CRC Press, Boca Raton, London, New York, Washington D.C. (2005).
5. *Carbon Nanotubes*, A. Jorio, G. Dresselhaus, and M.S. Dresselhaus (eds.), Springer-Verlag, Berlin, Heidelberg, New York (2008).
6. A. Szabo, C. Perri, A. Csato, G. Giordano, D. Vuono, and J.B. Nagy, *Materials* **3**, 3092 (2010).
7. S. Bellucci, *Phys. Status Solidi C* **2**, 34 (2005).
8. M. Endo, M.S. Strano, and P.M. Ajayan, *Potential Applications of Carbon Nanotubes*, *in: Carbon Nanotubes. Topics in Applied Physics*, A. Jorio, G. Dresselhaus, and M.S. Dresselhaus (eds.), Springer-Verlag, Berlin Heidelberg New York (2008).
9. M.F.L. De Volder, S.H. Tawfick, R.H. Baughman, and A.J. Hart, *Science* **339** (6119), 535 (2013).
10. *Industrial Applications of Carbon Nanotubes*, Huisheng Peng, Qingwen Li, and Tao Chen (eds.), Elsevier, Amsterdam, UK, US (2017).
11. W. Yi, L. Lu, Zhang Dian-lin, Z.W. Pan, and S.S. Xie, *Phys. Rev. B* **59**, R9015 (1999).
12. A. Mizel, L.X.Benedict, M.L. Cohen, S.G. Louie, A. Zettl, N.K. Budraa, and W.P. Beyermann, *Phys. Rev. B* **60**, 3264 (1999).
13. C. Masarapu, L.L. Henry, and B. Wei, *Nanotechnology* **16**, 1490 (2005).
14. G.A. Jorge, V. Bekeris, C. Acha, M.M. Escobar, S. Goyanes, D. Zilli, and R.J. Candal, *J. Phys.: Conf. Ser.* **167**, 012008 (2009).
15. G.A. Jorge, V. Bekeris, M.M. Escobar, S. Goyanes, D. Zilli, A.L. Cukierman, and R.J. Candal, *Carbon* **48**, 525 (2010).
16. A.N. Ponomarev, V.E. Egorushkin, N.V. Melnikova, and N.G. Bobenko, *Physica E* **66**, 13 (2015).
17. L.X. Benedict and S.G. Louie, and M.L. Cohen, *Solid State Commun.* **100**, 177 (1996).
18. V.B. Muratov, O.O. Vasil’ev, L.M. Kulikov, V.V. Garbuz, Y.V. Nesterenko, and T.I. Duda, *J. Superhard Materials* **34**(3), 173 (2012).
19. V.N. Popov, *Phys. Rev. B* **66**, 153408 (2002).
20. N.G. Bobenko, V.E. Egorushkin, N.V. Melnikova, A.A. Belosludtseva, L.D. Barkalov, and A.N. Ponomarev, *J. Struct. Chem.* **59**, 853 (2018).
21. N.G. Bobenko, V.E. Egorushkin, N.V. Melnikova, and A.N. Ponomarev, *Physica E* **60**, 11 (2014).
22. V.E. Egorushkin, N.V. Melnikova, A.N. Ponomarev, and A.A. Reshetnyak, *J. Phys.: Conf. Ser.* **248**, 012005 (2010).
23. M.S. Barabashko, A.E. Rezvanova, and A.N. Ponomarev, *Fullerenes, Nanotubes and Carbon Nanostructures* **25**, 661 (2017).
24. V. Egorushkin, N. Melnikova, A. Ponomarev, and N. Bobenko, *J. Mat. Sci. Eng. A* **1**, 161 (2011).
25. J. Hone, *Science* **289** (5485), 1730 (2000).
26. M.I. Bagatskii, M.S. Barabashko, A.V. Dolbin, V.V. Sumarokov, and B. Sundqvist, *Fiz. Nizk. Temp.* **38**, 667 (2012) [*Low Temp. Phys.* **38**, 523 (2012)].
27. M.I. Bagatskii, M.S. Barabashko, and V.V. Sumarokov, *Fiz. Nizk. Temp.* **39**, 568 (2013) [*Low Temp. Phys.* **39**, 441 (2013)].
28. M.I. Bagatskii, M.S. Barabashko, and V.V. Sumarokov, *Pis’ma v Zh. Èksper. Teoret. Fiz.* **99**, 532 (2014) [*JETP Lett.* **99**, 461 (2014)].
29. M.I. Bagatskii, V.V. Sumarokov, and M.S. Barabashko, *Fiz. Nizk. Temp.* **42**, 128 (2016) [*Low Temp. Phys.* **42**, 94 (2016)].

30. M.I. Bagatskii, M.S. Barabashko, V.V.Sumarokov, A. Jeżowski, and P. Stachowiak, *J. Low Temp. Phys.* **187**, 113 (2017).
31. V.L. Kuznetsov, S.N. Bokova-Sirosh, S.I. Moseenkov, A.V. Ishchenko, D.V. Krasnikov, M.A. Kazakova, and E.D. Obraztsova, *Phys. Status Solidi B* **251**, 2444 (2014).
32. A.I. Romanenko, O.B. Anikeeva, T.I. Buryakov, E.N. Tkachev, K.R. Zhdanov, V.L.Kuznetsov, I.N. Mazov, and A.N. Usoltseva, *Phys. Status Solidi B* **246**, 2641 (2009).
33. A.I. Romanenko, O.B. Anikeeva, T.I. Buryakov, E.N. Tkachev, K.R. Zhdanov, V.L. Kuznetsov I.N. Mazov, A.N. Usoltseva, and A.V. Ischenko, *Diamond & Related Materials* **19**, 964 (2010).
34. K.V. Elumeeva, V.L. Kuznetsov, A.V. Ischenko, R. Smajda, M. Spina, L. Forro, and A. Magrez, *AIP Adv.* **3**, 112101 (2013).
35. S.N. Bokova-Sirosh, V.L. Kuznetsov, A.I. Romanenko, M.A. Kazakova, D.V. Krasnikov, E.N. Tkachev, Y.I. Yuzyuk, and E.D. Obraztsova, *J. Nanophotonics* **10**, 012526 (2016).
36. V.L. Kuznetsov, K.V. Elumeeva, A.V. Ishchenko, N.Yu. Beylina, A.A. Stepashkin, S.I. Moseenkov, L.M. Plyasova, I.Yu. Molina, A.I. Romanenko, O.B. Anikeeva, and E.N. Tkachev, *Phys. Status Solidi B* **247**, 2695 (2010).
37. S.N. Bokova, E.D. Obraztsova, V.V. Grebenyukov, K.V. Elumeeva, A.V. Ishchenko, and V.L. Kuznetsov, *Phys. Status Solidi B* **247**, 2827 (2010).
38. *PPMS Manual–Heat Capacity Option User's Manual*, https://web.njit.edu/~tyson/PPMS_Documents/PPMS_Manual/1085–150%20Heat%20Capacity.pdf
39. A. Usoltseva, V. Kuznetsov, N. Rudina, E. Moroz, M. Haluska, and S. Roth, *Phys. Status Solidi B* **244**, 3920 (2007).
40. V.L. Kuznetsov, D.V. Krasnikov, A.N. Schmakov, and K.V. Elumeeva, *Phys. Status Solidi B* **249**, 2390 (2012).
41. I.N. Mazov, I.A. Ilinykh, V.L. Kuznetsov, A.A. Stepashkin, K.S. Ergin, D.S. Muratov, and J.-P. Issi, *J. Alloys Compounds* **586**, S440 (2014).
42. D. Szewczyk and A. Jeżowski, *J. Edu. Tech. Sci*. **2**, 22 (2015).
43. D. Szewczyk, A. Jeżowski, A.I. Krivchikov, and J.L. Tamarit, *Fiz. Nizk. Temp*. **41**, 598 (2015) [*Low Temp. Phys.* **41**, 469 (2015)].
44. T. Nihira and T. Iwata, *Phys. Rev. B* **68**, 134305 (2003).
45. T. Pérez-Castañeda, J. Azpeitia, J. Hanko, A. Fente, H. Suderow, and M.A. Ramos, *J. Low Temp. Phys.* **173**, 4 (2013).
46. M.G. Alexander, D.P. Goshorn, and D.G. Onn, *Phys. Rev. B* **22**, 4535 (1980).
47. O.O. Vasil'ev, V.B. Muratov, and T.I. Duda, *J. Super. Mat.* **32**, 375 (2010).
48. W. DeSorbo, *J. Chem. Phys.* **21**, 876 (1953).
49. A.N. Obraztsov, E.A. Obraztsova, A.V. Tyurnina, and A.A. Zolotukhin, *Carbon* **45**, 2017 (2007).
50. J.W. McClure, *Phys. Rev.* **108**, 612 (1957).
51. I.A. Gospodarev, V.I. Grishaev, E.V. Manzhelii, E.S. Syrkin, S.B. Feodosyev, and K.A. Minakova, *Fiz. Nizk. Temp*. **43**, 322 (2017) [*Low Temp. Phys.* **43**, 264 (2017)].
52. S. Rols, E. Anglare, J.L. Sauvajol, G. Coddens, and A.J. Dianoux, *Appl. Phys. A* **69**, 591 (1999).
53. S. Rols, Z. Benes, E. Anglaret, J.L. Sauvajol, P. Papanek, J.E. Fisher, G. Goddens, H. Schober, and A.J. Dianoux, *Phys. Rev. Lett.* **85**, 5222 (2000).
54. J.L. Sauvajol, E. Anglaret, S. Rols, and L. Alvarez, *Carbon* **40**, 1697 (2002).
55. B.A. Danilchenko, L.I. Shpinar, N.A. Tripachko, E.A. Voitsihovska, S.E. Zelensky, and B. Sundqvist, *Appl. Phys. Lett.* **97**, 072106 (2010).

Низькотемпературна питома теплоємність багатостінних вуглецевих нанотрубок

В.В. Сумароков, A. Jeżowski, D. Szewczyk, М.І. Багацький, М.С. Барабашко, А.Н. Пономарьов, В.Л. Кузнецов, С.І. Мосєєнков

Питому теплоємність багатостінних вуглецевих нанотрубок (БСВНТ) з низькою дефектністю та низьким вмістом неорганічних домішок виміряно в діапазоні температур 1,8–275 К методом теплової релаксації. Зразки БСВНТ отримано хімічним каталітичним осадженням з парової фази. Елементний склад і морфологію БСВНТ визначено за допомогою скануючої електронної мікроскопії та енергодисперсійної рентгенівської спектроскопії. Нанотрубки мали середній діаметр від 7 до 18 нм і довжину в кілька десятків мікрон. Чистота БСВНТ була більш ніж 99,4 ат.%. Маса зразків становила від 2 до 4 мг. Виявлено, що температурна залежність питомої теплоємності БСВНТ значно відрізняється від теплоємності інших вуглецевих матеріалів (графена, в'язок ОСВНТ, графіту, алмазу) при низьких температурах. Теплоємність БСВНТ систематично зменшується зі збільшенням діаметра нанотрубок при низьких температурах. Температурні залежності питомої теплоємності БСВНТ з різними діаметрами демонструють притаманний низьковимірним системам характер від 1D до 3D в залежності від температурних областей. Температури кросовера складають близько 6 та 40 К. Поблизу цих температур спостерігається гістерезис.

Ключові слова: вуглецеві нанотрубки, БСВНТ, питома теплоємність, низьковимірні системи.

Низкотемпературная удельная теплоемкость многостенных углеродных нанотрубок

В.В. Сумароков, A. Jeżowski, D. Szewczyk, М.И. Багацкий, М.С. Барабашко, А.Н. Пономарев, В.Л. Кузнецов, С.И. Мосеенков

Удельная теплоемкость многостенных углеродных нанотрубок (МСУНТ) с низкой дефектностью и низким содержанием неорганических примесей измерена в диапазоне температур 1,8–275 К методом тепловой релаксации. Образцы МСУНТ получены химическим каталитическим осаждением

из паровой фазы. Элементный состав и морфология МСУНТ определены с помощью сканирующей электронной микроскопии и энергодисперсионной рентгеновской спектроскопии. Нанотрубки имели средний диаметр от 7 до 18 нм и длину в несколько десятков микрон. Чистота МСУНТ более 99,4 ат.%. Масса образцов составляла от 2 до 4 мг. Обнаружено, что температурная зависимость удельной теплоемкости МСУНТ значительно отличается от теплоемкости других углеродных материалов (графена, связок ОСУНТ, графита, алмаза) при низких температурах. Теплоемкость МСУНТ систематически уменьшается с увеличением диаметра нанотрубок при низких температурах. Температурные зависимости удельной теплоемкости МСУНТ с разными диаметрами демонстрируют присущий низкоразмерным системам характер от 1D до 3D в зависимости от температурных областей. Температуры кроссовера составляют около 6 и 40 К. Вблизи этих температур наблюдается гистерезис.

Ключевые слова: углеродные нанотрубки, МСУНТ, удельная теплоемкость, низкоразмерные системы.